shows an abundance of *Densipollenites* and *Striatopodocarpites* is akin to Assemblage-RI-A (ref. 11), and the youngest assemblage in Patrapara, Assemblage-IV, is comparable to the Assemblage-RI-B (ref. 11), which represents *Striatopodocarpites* and *Crescentipollenites* prominence.

Besides the above-described quantitative structure, some forms which are qualitatively good age indicators are also present in these assemblages (Figure 3,*b–o*), viz. *Microfoveolatispora*, *Didecitriletes*, *Gondisporites*, *Densipollenites* spp., *Guttulapollenites*, *Mamealetus*, cf. *Playfordiaspora*, *Chordasporites* Klaus 1960 cf. *Lundbladispora*, cf. *Lunatisporites* and *Klausipollenites* Jansonius 1962. Cumulatively they confirm a late Late Permian age for these beds having equatability with Raniganj Formation.

Blanford *et al.*[2] recognized Talchir, Damudas and Mahadevas in the Talcher coal field. Their Damuda series included Barakar coal-measures which were supposed to be underlain by the strata referred to as Mahadevas, having a large stratigraphic break between the two[3]. Recently, Raja Rao[1] classified the lithostratigraphic sequence in Talcher coal field into Talchir, Karharbari and Barakar formations as Lower Permian and Kamthi Formation as Upper Permian–Triassic. The presence of Upper Permian Raniganj sequence in the area was also suggested by the megafossil findings of Subramanian (in Raja Rao[1]). The sediments of Kamthi Formation include fine- to medium-grained sandstone, carbonaceous shale, coal bands, greenish sandstone, pink clays and pebbly sandstone at the top (total thickness 250 m). The section exposed at Patrapara fits in the circumscription of the coal–shale–clay package of Kamthi Formation given by Raja Rao[1], although in the map he included this part of the area in the Barakar Formation.

In addition to the Patrapara section, a preliminary palynological study of the uppermost coal–shale sequence in bore hole TCW-6 drilled in the central part of the field between Kosala and Kukurpeta reveals a correlation between the Patrapara section and the depth levels 290.92 m and 303.72 m. The palynozone recognized at the latter depths contains, besides striate pollen, *Klausipollenites*, *Crescentipollenites* and *Densipollenites* in frequency comparable with that in the Patrapara assemblages. Additionally, the most revealing support for a Late Permian age of the TCW-6 palynozone under consideration is the presence of the taxa *Guttulapollenites*, *Satsangisaccites*, *Chordasporites*, *Alisporites* and *Osmundacidites*. In view of this the presence of latest Permian sediments can be envisaged in a wider extent of the western part of the Talcher coal field.

In the Patrapara section the coal–shale–clay beds—having a latest Permian age affinity—and the gritty coarse-grained sandstone resting on its highly denuded surface suggest a considerable gap between the coal-bearing strata and the Mahadevas. The presence of Lower Triassic Panchet Formation is indicated in bore hole TCW-6 where a thick profile of green and chocolate facies overlies the coal–shale facies; the latter contains Upper Raniganj palynoflora. Thus the presence of Raniganj, Panchet and Mahadeva formations *sensu* Subramanian and Chakraborty and Das and Banerjee (in Raja Rao[1])—combinedly designated as Kamthi Formation by Raja Rao[1]—is corroborated by identifying the uppermost Permian sequence on the basis of palynology.

The western part of the Talcher coal field is thus a highly promising area for exploring the subsurface Upper Permian coals.

1. Raja Rao, C. S., *Bull. Geol. Surv. India Ser.* A, 1982, **45**, 41.
2. Blanford, W. T., Blanford, H. T. and Theobald, W., *Mem. Geol. Surv. India*, 1856, **1**, 33.
3. Fox, C. S., *Mem. Geol. Surv. India*, 1934, **58**, 162.
4. Venkatachala, B. S. and Tiwari, R. S., *Palaeobotanist*, 1988, **36**, 24.
5. Tiwari, R. S., *Geophytology*, 1974, **4**, 111.
6. Rana, V. and Tiwari, R. S., *Geophytology*, 1980, **10**, 108.
7. Tiwari, R. S. and Rana, V., in *Proc. Symp. Evolution. Biostratigr* (eds. Sharma, A. K. *et al.*), A. K. Ghosh Commemoration Volume, Today and Tomorrow's Printers and Publishers, New Delhi, 1984, p. 425.
8. Tiwari, R. S., Srivastava, S. C., Tripathi, A. and Singh, V., *Geophytology*, 1981, **11**, 220.
9. Tiwari, R. S. and Ram-Awatar, *Palaeobotanist*, 1989, **37**, 94.
10. Srivastava, S. C. and Jha, N., *Palaeobotanist*, 1989, **37**, 199.
11. Tiwari, R. S. and Singh, V., *Bull. Geol. Min. Metall. Soc. India*, 1986, **54**, 256.
12. Tiwari, R. S. and Tripathi, A., *Palaeobotanist*, 1988, **36**, 87.

ACKNOWLEDGEMENTS. We are grateful to the Director, Coal Division, Geological Survey of India, Calcutta, for providing support in various ways to our efforts for palynodating of Gondwana coals. Thanks are also due to the Director, GSI, Coal-Division-II, Sri S. K. Sahay, and the Senior Geologist of the Talcher Coalfield, Sri P. K. Mohanty, for their kind help and keen interest in the collection of samples.

15 October 1990; revised accepted 18 February 1991

The crystal and molecular structure of putrescine–DL-glutamic acid complex

S. Ramaswamy and M. R. N. Murthy
Molecular Biophysics Unit, Indian Institute of Science, Bangalore 560 012

The polyamines spermine, spermidine, putrescine, cadaverine, etc. have been implicated in a variety of cellular functions. However, details of their mode of interaction with other ubiquitous biomolecules is not known. We have solved a few structures of polyamine–amino acid complexes to understand the nature and mode of their interactions. Here we report the structure of a complex

of putrescine with DL-glutamic acid. Comparison of the structure with the structure of putrescine–L-glutamic acid complex reveals the high degree of similarity in the mode of interaction in the two complexes. Despite the presence of a centre of symmetry in the present case, the arrangement of molecules is strikingly similar to the L-glutamic acid complex.

EVEN after extensive research on the structure and interactions of the naturally occurring polyamines such as spermine, spermidine, putrescine and cadaverine[1], their specific function is still obscure. However, their ubiquitous distribution and participation in a wide variety of functions have stimulated many investigations on these compounds. They have been shown to interact with DNA[2], RNA[3], proteins[4] and membrane components[5]. The most pressing questions in the polyamine field are concerned with their physiological role and the molecular mechanisms of their action. Our attempts to answer the latter question led us to investigate the three-dimensional structure of a number of complexes of polyamines with amino acids by techniques of single-crystal X-ray diffraction. We have determined the structures of putrescine complexed with L-glutamic acid[6] and L-aspartic acid[7], propane diamine complexed with L-glutamic acid and DL-glutamic acid (unpublished results), hexane diamine with L-glutamic acid[8], and putrescine with DL-glutamic acid. Here we report the structure of the complex of putrescine with DL-glutamic acid. The interactions in the present case are similar to those in the putrescine–L-glutamic acid complex. Surprisingly, minor changes in conformation of L-glutamic acid are sufficient to provide a similar environment for putrescine.

Crystals of a 2:1 complex of DL-glutamic acid and putrescine were obtained from aqueous solution by liquid diffusion of propanol. The crystals belong to the monoclinic space group $P2_1/n$, with $a = 5.231(1)$ Å, $b = 22.815(2)$ Å, $c = 7.858(1)$ Å, $\beta = 93.34°$. The volume of 936.3(2) Å^3 suggests that there are one glutamic acid and half a putrescine in the crystal asymmetric unit. This leads to a calculated density of 1.36 g cm^{-3}.

X-ray diffraction data were collected on an Enraf Nonius 4 circle diffractometer using CAD4 geometry. A microfocus sealed tube equipped with a molybdenum anode ($\lambda = 0.7107$ Å) was used as the X-ray source. A total of 1965 reflections were collected, out of which 1011 were unique. The quality of the reflection data is reflected in the R-factor of 3.8% between the symmetry-equivalent reflections. Periodically monitored intensity control reflections showed no radiation damage to the crystal during data collection. The reflection intensities were corrected for Lorentz and polarization factors but not for absorption.

The structure was solved using the direct-methods program SHELEX 86. Structure was refined by the full matrix method using the program SHELEX 400. The non-hydrogen atoms were refined unisotropically. All the hydrogen atoms were located from difference Fouriers and subsequently refined isotropically. The final R factor at the end of refinement was 6.2% for $|F(o)| \geq 5\sigma|F(o)|$. The difference Fourier at the end of refinement has a maximum electron density of less than 0.5 electrons per Å^3.

The atomic coordinates and temperature factors of all the non-hydrogen atoms in the asymmetric unit have been submitted as supplementary material with the journal. Table 1 gives a list of bond lengths and bond angles. Table 2 compares the conformation of glutamic acid in different structures. This table suggests that the glutamic acid in the present case is in a conformation similar to that in the putrescine–L-glutamic acid complex. Similarly the conformation of putrescine is also conserved between the two structures. Further, the two complexes also have very similar hydrogen-bonding patterns, as shown in Table 3.

Although the present structure has striking resemblance to that of the putrescine–L-glutamic acid complex, the crystallographic asymmetric unit is only half that of the latter. The asymmetric unit contains one glutamic acid and half a putrescine, in contrast to the

Table 1. Bond lengths and bond angles.

Bond distances (Angstrom)
(Corrections following Busing and Levy, *Acta Crystallogr.*, 1964, **17**, 142)

Bond	Uncorrected distance	Lower bound	Upper bound	Riding motion	Noncorrelated motion
N1–C2	1.4740 (94)	1.4743	1.5706	1.4786	1.5224
O1–C1	1.2395 (83)	1.2419	1.3551	1.2560	1.2985
O2–C1	1.2558 (83)	1.2579	1.3664	1.2711	1.3122
C1–C2	1.5345 (112)	1.5352	1.6361	1.5433	1.5857
C2–C3	1.5108 (100)	1.5117	1.6552	1.5226	1.5835
C3–C4	1.4972 (120)	1.4976	1.6539	1.5043	1.5758
C4–C5	1.5782 (109)	1.5793	1.7100	1.5900	1.6446
C5–O6	1.2073 (97)	1.2112	1.4244	1.2363	1.3178
C5–O7	1.2296 (83)	1.2330	1.4456	1.2569	1.3393
N11–C12	1.4749 (91)	1.4751	1.5534	1.4788	1.5143
C12–C13	1.4918 (89)	1.4920	1.5713	1.4958	1.5316

Bond angles (Degrees)
(ESD following Cruickshank, International Tables II, 1959, p. 331)

	Angle	ESD
O1–C1–O2	125.17	0.63
O2–C1–C2	119.50	0.60
O1–C1–C2	115.24	0.61
N1 C2 C1	109.51	0.57
C1–C2–C3	113.07	0.64
N1–C2–C3	114.98	0.62
C2–C3–C4	110.77	0.67
C3–C4–C5	112.24	0.69
C4–C5–O7	112.42	0.61
C4–C5 O6	124.71	0.64
O6 C5 O7	122.61	0.64
N11 C12 C13	111.34	0.55

Table 2. Comparison of torsion angles of different glutamic acid forms.
(All angles are in degrees)

Torsion angle	x-Form	β-Form	Protonated	Complex 1 Glu 1	Complex 1 Glu 2	Complex 2 Glu 1	Complex 2 Glu 2	Complex 3 Glu
N-C-C-O(1)	−50	−42	161	168	156	134	−12	161
N-C-C-O(2)	130	141	−21	−11	−24	−43	166	−22
N-C-C-C	178	−51	−69	65	63	178	73	67
C-C-C-C	68	−73	−173	−179	175	71	−71	171
C-C-C-O(6)	74	19	15	9	−53	−171	10	15
C-C-C-O(7)	−105	−161	−167	176	128	14	−170	−171

Errors in angles are of the order of one degree.

Complex 1: putrescine–L-glutamic acid
Complex 2: hexane diamine–L-glutamic acid
Complex 3: putrescine–DL-glutamic acid

Table 3. Possible hydrogen bonds

Donor–H	Donor···Acceptor	H···Acceptor	Donor–H···Acceptor
N1 –H1N1	N1 ···O1 (1)	H1N1 ···O1 (1)	N1 –H1N1···O1 (1)
0.965 (.078)	2.851 (.008)	1.974 (.077)	149.88 (6.23)
N1 –H2N1	N1 ···O6 (2)	H2N1···O6 (2)	N1 –H2N1···O6 (2)
1.074 (.090)	2.734 (.009)	1.717 (.085)	156.13 (6.93)
N1 –H3N1	N1 ···O7 (3)	H3N1···O7 (3)	N1 –H3N1···O7 (3)
1.136 (.071)	2.749 (.007)	1.645 (.071)	162.37 (5.98)
N11 –H1N2	N11 ···O7 (0)	H1N2···O7 (0)	N11 –H1N2···O7 (0)
0.783 (.051)	2.749 (.008)	2.065 (.054)	145.88 (5.00)
N11 –H2N2	N11 ···O1 (4)	H2N2···O1 (4)	N11 –H2N2···O1 (4)
0.871 (.055)	2.805 (.007)	1.963 (.054)	162.23 (5.12)
N11 –H3N2	N11 ···O2 (5)	H3N2···O2 (5)	N11 –H3N2···O2 (5)
0.994 (.073)	2.834 (.008)	1.853 (.073)	168.73 (5.07)

Equivalent positions:

(0) X, Y, Z
(1) $+X-1, +Y, +Z$
(2) $+X-1/2, -Y+1/2+1, +Z+1/2$
(3) $+X, +Y, +Z+1$
(4) $+X-1, +Y, +Z-1$
(5) $-X+1, -Y+2, -Z+1$

complex with L-glutamic acid where the asymmetric unit contains two glutamic acid and one putrescine molecules. This difference is mainly due to the presence of an inversion centre in the present case. In the complex of putrescine with L-glutamic acid, where the inversion symmetry is forbidden, two crystallographically distinct L-glutamic acids are present. The major difference in the conformation of these two glutamic acids is confined to the orientation of the side-chain carboxyl groups. This difference is presumably due to the packing forces derived from hydrogen bonding.

Comparison of the packing diagrams of the DL-glutamic acid (Figure 1) and the L-glutamic acid (Figure 2) complexes shows striking similarities. Both crystals consist of sheets of putrescine sandwiched between layers of glutamic acid. All the central carbon atoms of putrescine are involved in van der Waals interactions. This is the major interaction stabilizing sheets of putrescine parallel to the *ac* plane. The terminal amino groups of putrescine are neutralized by layers of carboxylate groups. There are two distinct sheets of glutamic acid molecules parallel to the *ac* plane of putrescine in the putrescine–L-glutamic acid complex. In the present case also, two layers of glutamic acid molecules exist. However, the two layers consist of chirally distinct molecular species of glutamic acid and are related by the crystal centre of symmetry. The layers are stabilized by extensive van der Waals contact between nonpolar atoms of glutamic acid

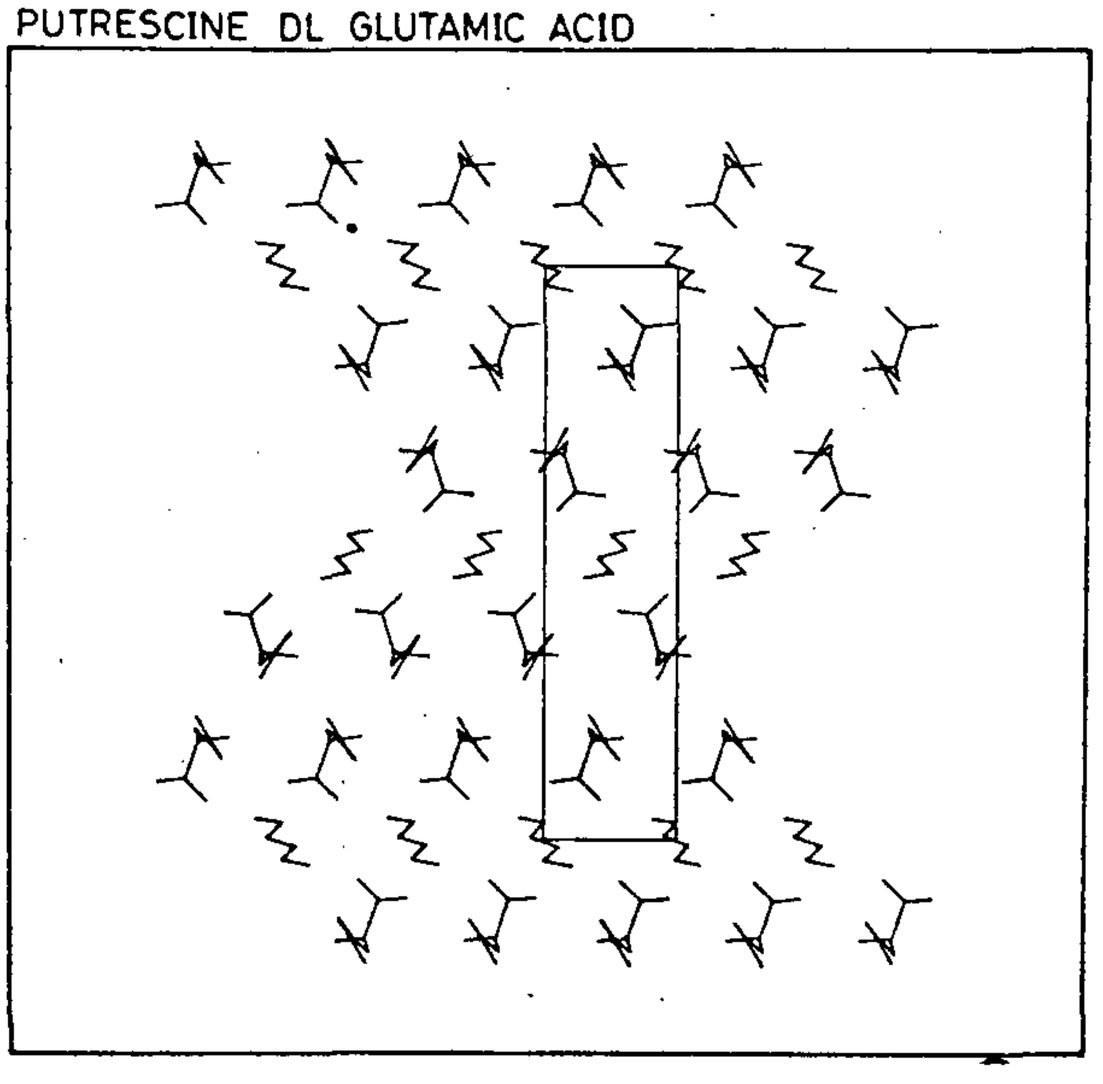

Figure 1. Packing diagram of putrescine–DL-glutamic acid complex.

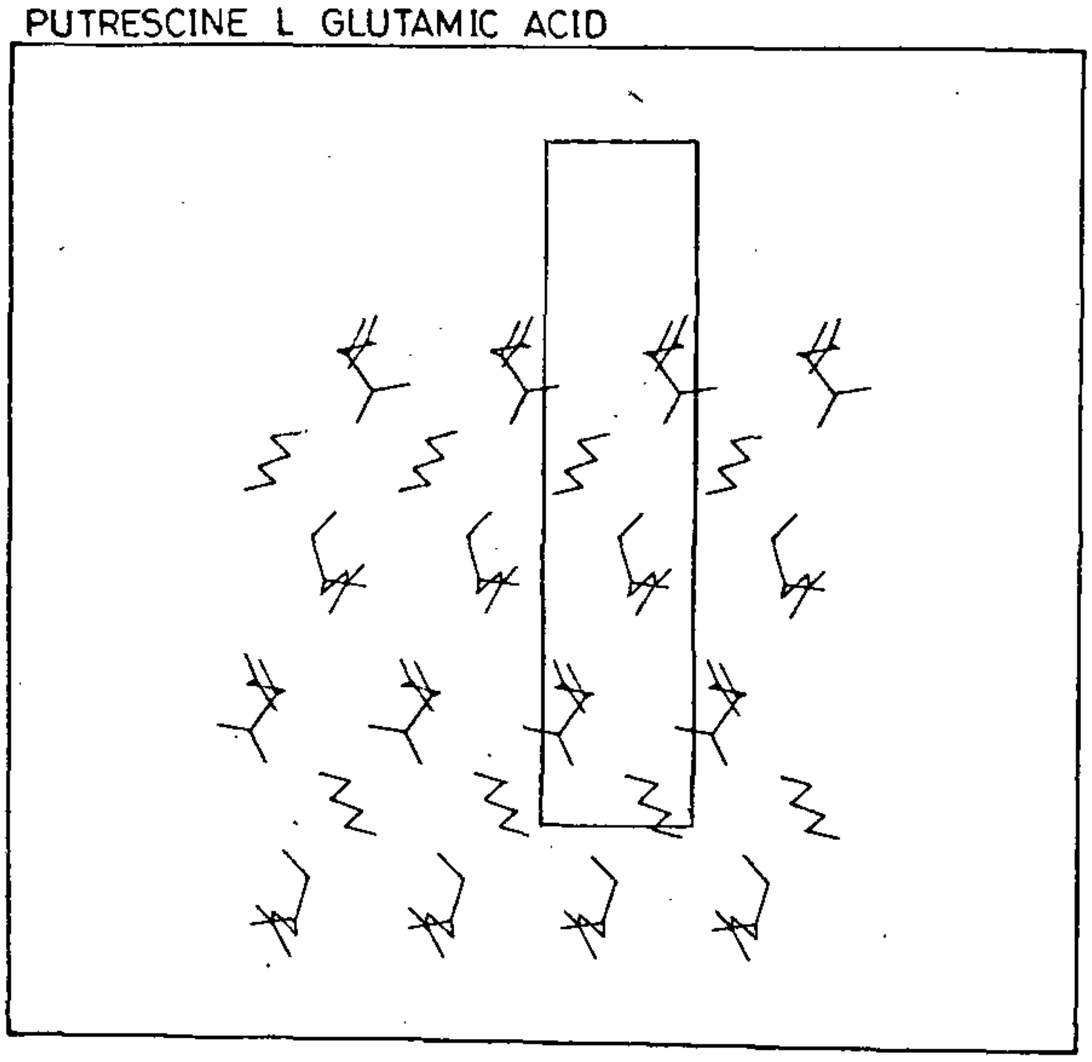

Figure 2. Packing diagram of putrescine–L-glutamic acid complex.

molecules along the *a* axis. Also, there is a continuous chain of hydrogen bonds between the main-chain carboxyl and main-chain amino groups along *a*. The layers are additionally stabilized by hydrogen bonding between main- and side-chain carboxylates and putrescine amino groups. The two layers of D and L glutamic acid molecules sandwiched between putrescine layers are held together by hydrogen bonding between side-chain carboxyl groups and main-chain amino groups. A comparison of the two complexes suggests that the conformation of putrescine and the pattern of packing and hydrogen bonding are conserved, although the chemical environments surrounding the putrescine are different. The putrescine has retained its most-favourable *trans* conformation in both structures. The conformational flexibility of the glutamic acid side chains accounts for the similarities of packing environment and conservation of polyamine conformation in the structures.

1. Tabor, C. W. and Tabor, H., *Annu. Rev. Biochem.*, 1984, **53**, 749.
2. Frederick, C. A., Williams, D. L., Giovanni, U., Van der Marel, G. A., Van Boom, J. H., Rich, A. and Wang, A. H. J., *Biochemistry*, 1990, **29**, 2538.
3. Gary, J. Q., Martha, M. T. and Rich, A., *Proc. Natl. Acad. Sci. USA*, 1978, **75**, 64.
4. Frederick, G. W., Jr. and Kitareewan, S., *J. Biol. Chem.* 1990, **265**, 7127.
5. Smith, T. A., *Annu. Rev. Plant Physiol.*, 1985, **36**, 117.
6. Ramaswamy, S., Nethaji, M. and Murthy, M. R. N., *Curr. Sci.*, 1989, **58**, 1160.
7. Ramaswamy, S. and Murthy, M. R. N., *Curr. Sci.*, 1990, **59**, 379.
8. Ramaswamy, S. and Murthy, M. R. N., *Curr. Sci.*, 1991, **60**, 173.

ACKNOWLEDGEMENTS. M.R.N.M thanks CSIR for financial assistance. S.R. is a UGC senior research fellow.

Received 21 February 1991; accepted 3 April 1991

Uptake, binding and photodynamic action of haematoporphyrin derivative in brain tumour cells

Kunju Joshi, Preeti G. Joshi and Nanda B. Joshi

Department of Biophysics, National Institute of Mental Health and Neuro Sciences, Bangalore 560 029, India

The photosensitizer haematoporphyrin derivative (Hpd) is a mixture of various monomeric forms of porphyrins such as haematoporphyrin (HP), protoporphyrin (PP), hydroxyvinyldeuteroporphyrin and a covalently linked aggregated form known as dihaematoporphyrin ester/ether (DHE). Hpd, in combination with light, is used in the diagnosis and treatment of cancer. We have studied uptake, binding and photodynamic action of Hpd in brain tumour cells. Hpd uptake by cells increased with increase in Hpd concentration in medium as well as with increase in incubation time; the cells were more photosensitive in the latter case. Fluorescence intensity of cell-bound Hpd increased with increased uptake by the cells. Upon prolonged incubation, the fluorescence emission spectrum of cell-bound Hpd showed changes in the position of one peak and relative intensities of the peaks. Our data suggest that the increase in photodynamic cellular damage on prolonged incubation may be due to increased accumulation of aggregated ester/ether component of Hpd and/or binding of Hpd to specific sites in the cell.

PHOTODYNAMIC therapy (PDT) for cancer[1-3] is based on bringing about selective accumulation of Hpd by tumour tissue followed by irradiation with light. The fluorescence emitted by tumour-bound Hpd serves for detection while laser irradiation of Hpd-containing tumour is used for the treatment. It has been proposed that, in photodynamic action, the excited photosensitizer may transfer electrons to the surrounding biomolecules with the formation of free radicals, or transfer energy to oxygen leading to the formation of highly reactive singlet oxygen[4,5]. It has been shown that the photodynamic action of Hpd on cells in culture is higher when cells are incubated for longer times before irradiation but the exact cause of this is not yet known[6-8]. In an attempt to understand the cause of this enhanced photodamage, we have studied uptake, binding of Hpd by brain tumour cells and photosensitization of the cells.

Hpd was prepared from haematoporphyrin dihydrochloride (Sigma) by the method of Lipson *et al.*[9] BMG-1 cells were grown in Nunc plastic tissue culture flasks using Dulbecco's minimum essential medium (DMEM; Hi-Media) supplemented with 5% bovine serum and